

An Assessment of a Method for Designing Polymer-Based Composite Materials for Radiation Phantoms

Edward R. Long, Jr.
Longhill Technologies inc.

Abstract.

1. INTRODUCTION

The human body is a composition of approximately 36 elements, Ref 1, some in abundance and others in trace amounts. The elemental composition is not the same for all parts of the body. Bone's constituents are different from that of non-structural tissue and for the latter the composition varies from one type tissue to another. These differences are important for radiation-related medical purposes because each element absorbs radiation energy more or less differently and hence so does the particular portion of the body in question. This has been recognized and the differences and near-approximate constituencies of human tissues have been documented, Ref 2.

The ICRU report, Ref 2, presents plastic formulations whose radiation absorptions were felt to be near those of bone and various tissues for medical radiation-related research and treatment. Plastic-based materials are used extensively for the construction of medical radiation phantoms and build-up caps, partly because of determinations such as Ref 2. However, as has been recently demonstrated for build-up caps, Ref 3, non-plastic materials, such as brass, can be used. Brass and other higher-Z materials appear to be used for build-up caps because of their relatively small geometry for high-MV photon sources, such as from 15- to 25-MV photon spectra. On the other hand, the materials used for phantoms are somewhat more critically chosen because the need for quantitative emulation of volume as well as radiation absorption of the human body for clinical treatment and medical research.

Several polymeric materials are used today in their neat-form for human-tissue phantoms, amongst which are polyethylene (PE), polymethylmethacrylate (PMMA), and epoxies of various functionalities and cross-linking activators. In some cases combinations of these and other polymers, and non-organic fillers, as in the case of Shonka's A-150 tissue-equivalent plastic, Ref 4, are used. There are other polymeric formulations that are specific to a particular type tissue, such as A-181 brain-equivalent plastic, Ref 5. However, as the specificity of radiation treatment of human tissue becomes more precise, both locative and quantitative, questioning of the accuracy in using these materials will become more important. A combination of two avenues for a suitable solution would appear possible: design materials that more accurately represent the absorption performances of human tissues or develop accurate transformation matrix tables that eliminate the remaining discrepancies of the new materials.

In this paper we briefly discuss an application we have developed for matching blends of polymeric and inorganic materials to that of a reference tissue material. We then discuss the dose characteristics of two tissue-equivalent blends that we formulated using the application. These could guide the choice of methods for future tissue-equivalent developmental studies in the light of Monte Carlo modeling which we also performed for the two blends. The reference tissue material we employed was ICRU44 Soft Tissue; however, the approach in this study should perform equally as well using standards for other tissue-based materials, such as for bone and brain.

2. METHOD AND MATERIALS

2.1 Method

We developed a simple application that employs NIST photonic energy absorption data for atomic elements to determine the absorption characteristics of molecular and blended composite structures and to compare the net absorption parameters of any two or more to that of standards, Ref 1- 5. The comparison aspect of the application utilizes an iterative approach that causes the formulated polymeric blend's spectral absorption properties to converge towards those of a reference tissue material, in this case ICRU44 Soft Tissue, hereafter termed simply as 'ICRU44'. We used the application to examine, in all, more than 50 2-polymer, 3-polymer, and 4-polymer blends, with and without as many as 4 inorganic additives. In each case we determined the ratios for best-match with ICRU44.

The Monte Carlo tool EGSrz was used to examine the depth-dose characteristics of the convergent formulated blends and ICRU44, as well as several neat resins and A150 Tissue Equivalent Plastic, hereafter termed simply 'A150', for two spectral-distributions of photon radiation. The primary purpose for using the MC tool was to evaluate the merit of our simple absorption application for material development.

Default values were used for the MC tool's Transport and Variance Parameters. For each photon spectra a sufficient number of histories were determined, prior to the actual data runs, to insure error of 0.1 percent or less. The geometry was kept as simple as possible, two Ring Zones and 60 Planar Zones (slabs) as depicted in Figure 1. A parallel, normally-incident beam was used.

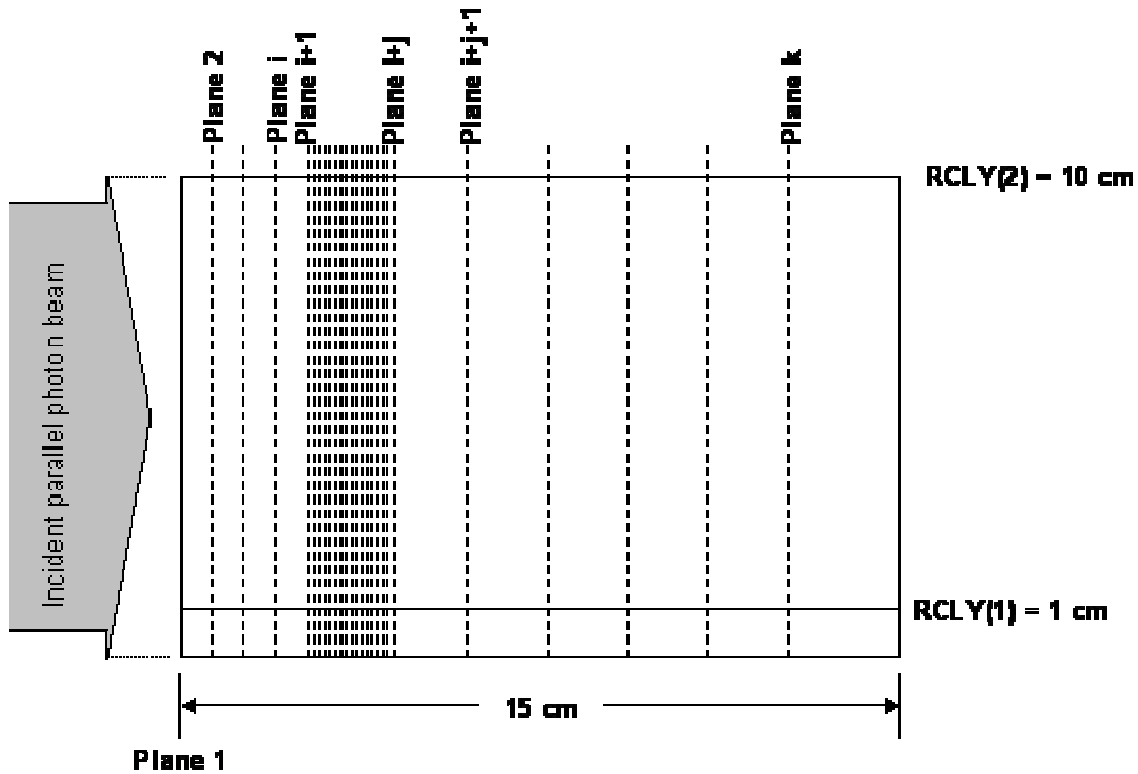


Figure 1 – Monte Carlo modeled exposure geometry using EGSrz

For each photon spectral energy distribution the values for i , j , and k and for the widths of the respective slabs were selected to yield a depth dose profile for which the maximum dose was within the group of planes from i to j , with reasonable special resolution for each slab within this group, and for which there were a sufficient number of slabs to depict the depth dose profile before and after. It may be argued that something other than an incident parallel beam would have been appropriate but for simplicity, and a reasonable run time, the particular beam was chosen. Data were recorded for the inner region under the assumption that for the range of photon energies studied reasonable dose equilibrium would occur.

Depth-Dose profiles were determined for spectral-energetic photons corresponding to Cobalt 60 and Mohan 15 sources, the spectra for which are embedded in the EGSrz tool. Mohan 15 refers to the spectra of a 15-MV photon source determined by Mohan using EGS3, Ref 6. The electronic-composition was not included in this study.

2.2 – Materials

The materials modeled were ICRU44, PE, PMMA, A150, and two optimized tissue-equivalent polymeric blends of polymers, TEPB1 and TEPB2. For this work ICRU44, Ref 2, was assumed to be the standard representing soft tissue to which polymer-based synthetic tissue materials are compared. PE and PMMA are two popular neat-resin thermoplastics frequently used for phantoms, Ref 7 - 11. There are multiple reasons for their popularity, including availability and fairly good representation of human tissue,

especially considering that neither of the two were originally developed for phantom purposes.. A150 is a polymer blend that is frequently used in ionization chambers and phantoms, Ref 12 – 16. It is a well-known, established, widely-used multiple-polymer representation of tissue. As for all plastic-based materials, the problem with A150 is the differences of its carbon and oxygen content compared to that of soft tissue. However the two elements have similar absorption characteristics and with addition of inorganic additives, such as calcium fluoride, Shonka was able to develop a material that could be molded and machined and that was stable. TEPB1 is a 3-polymer blend with inorganic additives and TEPB2 is a 4-polymer blend with no inorganic additive.

3. RESULTS AND DISCUSSION

3.1 – Materials and Modeling

TEPB1 and TEPB2 are the two best matches we found. TEPB1 is a blending of three resin systems and an inorganic additive. TEPB2 is a blending of four resin systems. Spectral absorption data from our simple application and depth-dose data from Monte Carlo modeling for the 6 materials are presented and discussed.

3.2 – Absorption

Table I lists the percent difference of the materials’ absorption for photon energies, from 1 keV to 20 MeV. We have divided the spectral span into three ranges, low- (0.001 MeV – 0.080 MeV), mid- (0.100 MeV – 1.5 MeV), and high-range (2.0 MeV – 20.0 MeV). PE’s absorption differs 10 % or more from that of ICRU44 ni all three ranges. PMMA’s absorption differs 10 % or more for all but a small portion of the top portion of the low-range and the top portion of the high-range for which it is as small as 6 %. A150’s difference with that fo ICRU44 is between that for PE and PMMA at the very bottom portion of the low-range but otherwise is significantly smaller than either of the two neat resins. From the values in this table it should be noted that a 50/50 combination of PE and PMMA provides good agreement with ICRU44 for photon energies from 0.15 MeV to 4.00 MeV.

Table I – % difference of materials’ absorption from that of ICRU44-Soft Tissue

Energy (MeV)	% Diff wrt ICRU44 μ_a , 1/cm)					Energy (MeV)	% Diff wrt ICRU44 μ_a , 1/cm)				
	PMMA	PE	A150	TEPB1	TEPB2		PMMA	PE	A150	TEPB1	TEPB2
0.001	-17.82	-55.71	-35.28	-36.99	-39.49	0.200	10.49	-10.43	5.92	-0.20	1.39
0.002	-20.46	-58.38	-38.11	-39.43	-41.52	0.300	10.74	-10.15	6.08	-0.04	0.83
0.002	-21.74	-59.79	-39.52	-40.65	22.64	0.400	10.72	-10.12	6.06	-0.05	0.58
0.003	-27.79	-63.40	-44.11	-44.96	25.60	0.500	10.79	-10.05	6.12	0.00	0.54
0.004	-31.60	-65.53	-46.84	-47.57	26.87	0.600	10.81	-10.03	6.13	0.02	0.50
0.005	-32.63	-66.24	-22.76	-29.63	30.05	0.800	10.80	-10.03	6.12	0.01	0.44
0.006	-33.32	-66.66	-21.50	-28.77	32.51	1.000	10.80	-10.04	6.10	0.00	0.41
0.008	-34.08	-66.89	-19.26	-27.17	35.73	1.250	10.81	-10.02	6.12	0.01	0.41
0.010	-33.97	-66.32	-17.26	-25.62	37.70	1.500	10.83	-10.02	6.14	0.02	0.43
0.015	-30.94	-61.93	-12.75	-21.66	48.60	2.000	10.71	-10.21	5.98	-0.12	0.38
0.020	-25.15	-54.49	-8.68	-17.56	44.63	3.000	10.46	-10.70	5.65	-0.44	0.35
0.030	-11.87	-38.01	-2.33	-10.42	30.48	4.000	10.16	-11.29	5.25	-0.84	0.33
0.040	-2.54	-26.56	1.31	-6.02	18.88	5.000	9.84	-11.92	4.82	-1.26	0.30
0.050	2.71	-20.10	3.21	-3.66	11.88	6.000	9.49	-12.59	4.37	-1.70	0.26
0.060	5.62	-16.53	4.22	-2.37	7.89	8.000	8.86	-13.87	3.50	-2.55	0.20
0.080	8.29	-13.21	5.14	-1.20	9.50	10.000	8.20	-15.10	2.63	-3.39	0.09
0.100	9.39	-11.85	5.53	-0.70	5.81	15.000	6.98	-17.56	0.96	-5.03	-0.03
0.150	10.26	-10.74	5.84	-0.31	2.42	20.000	6.00	19.47	-0.34	6.30	-0.15

TEPB1 provides almost three orders-of-magnitude better agreement with ICRU44 for the mid-range energy values that does either of the two neat resins, and almost as much improvement with respect to A150. (Note: It is an order of magnitude better agreement than that provided by a 50/50 mix of PE and PMMA.) For the low-range its values are in better agreement than those of PE and about the same as those for PMMA and A150. From these absorption data TEPB1 might be expected agree well with human soft tissue for Co-60 radiation. In the high-range it is also somewhat better than either of the two neat resins but far short of that of A150. Thus, from these data it might not be expected to provide phantom performance as well as does A150 for the X-ray sources used for cancer treatment unless the spectral distribution is small above 8-MeV.

TEPB2 provides a little more than an order of magnitude better agreement with ICRU44 than both neat resins and A150 for energy values down to 0.150 MeV. For energy values less than 0.150 MeV it provides no better agreement than that of the two neat resins and not as good as A150. However, for the high range of energies it is significantly better than the two neat resins and A150. Thus TEPB2 might be expected to provide excellent phantom performance for X-ray sources of radiation used for cancer treatments.

Several general conclusions can be made from the data: (1) Tissue-equivalent blends of polymers and inorganic additives are possible that provide much better agreement with the absorption of photonic energy by soft tissue than the current standard A150 and far better than the neat resins that are popular as phantom material. (2) While no one mix matches the absorption properties of soft tissue for the entire spectra, from 1 keV to 20 MeV, it is possible to tailor mixes for narrow ranges that are specific to types of radiation, such as Co60 which is used for Gamma Knife and X-Rays from linear accelerators that are used for teletherapy. (3) Neither the neat resins or blends appear to agree well with soft tissue's absorption for the low-range energy.

There is however a question for how well the depth-dose data for these blends agree with that of ICRU44. Intuitively the answer is that this agreement should correspond to that of the absorption data; however, there are aspects, such as the poorer agreement at the low-range energies that cloud the sense of intuition. The answer requires determination of depth-dose data, such as provided by available MC tools. If the depth-dose data substantiates the conclusions made from the absorption data then it is readily apparent using elemental absorption data is a far more cost-effective method for developing phantom material blends that optimally match the various types of tissues for specific ranges of photon energies.

3.3 – Monte Carlo Modeled Depth-Dose Data

Figure 2 provides for a comparison of the depth-dose profiles of PE and PMMA to that of ICRU44 for (a) Co60 and (b) Mohan15 photon spectra. For all of the depth-dose plots in this paper the dose values are normalized to that of ICRU44's which occurs due to build-up.

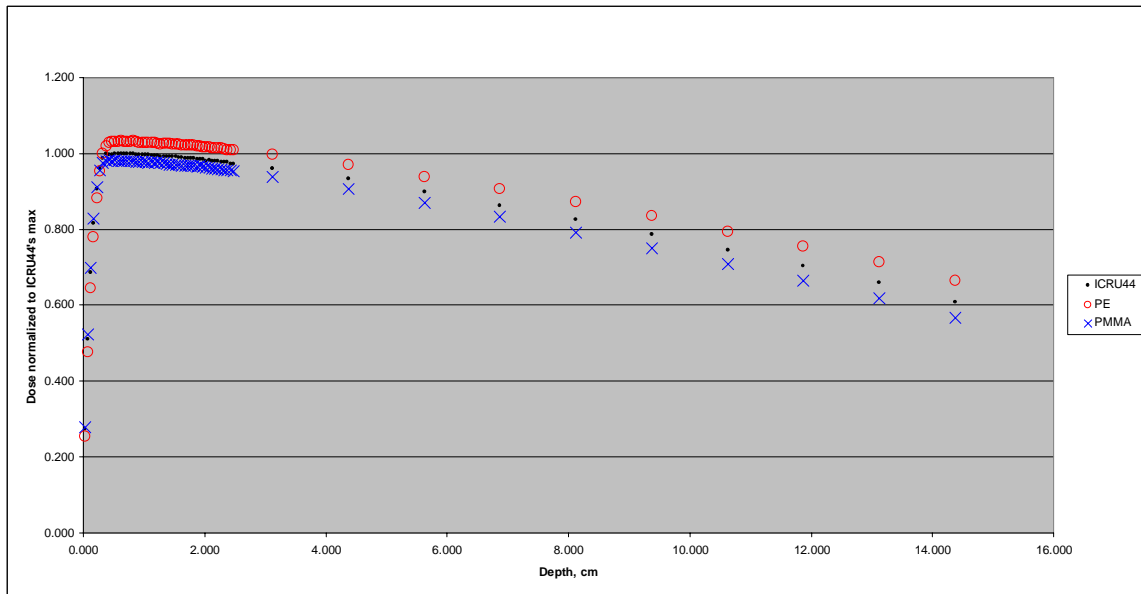


Figure 2a – Depth-dose profiles of ICRU44, PE, and PMMA for Co60 photons

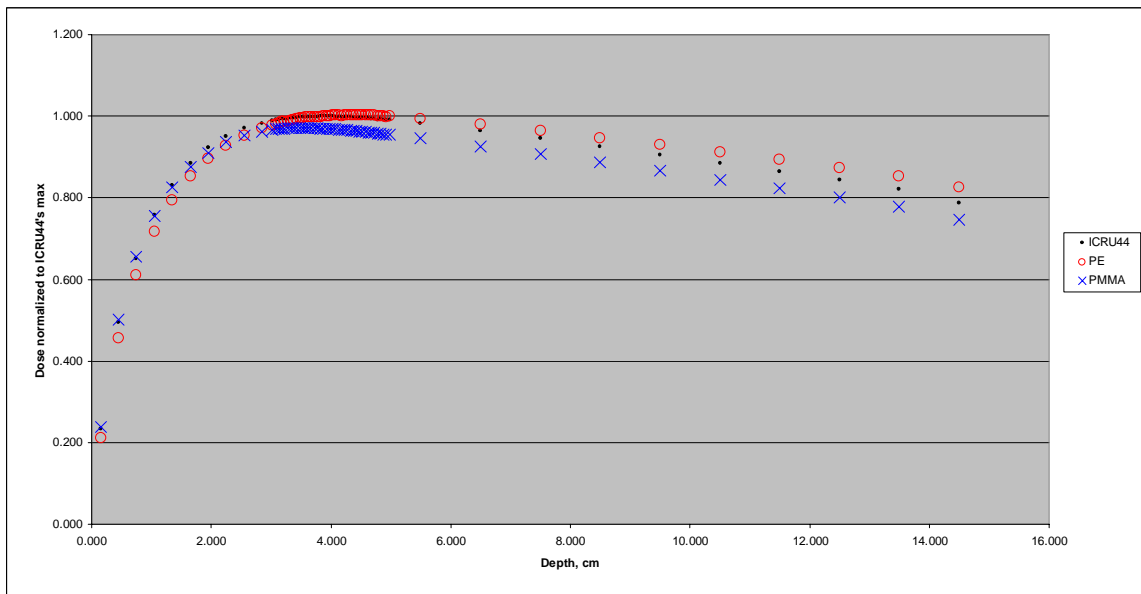


Figure 2b – Depth-dose profiles of ICRU44, PE, and PMMA for Mohan15 photo

Perhaps the clearest explanation for why PMMA's dose at a shallow depth is more and at larger depth is less than that of ICRU44's is to cite a mono-energetic case, such as shown in Figure 3 for a 1.25-MeV photon. At 1.25-MeV, PMMA's absorption is higher than that of ICRU44's by approximately 11 %, see Table I. Thus the dose from PMMA is expected to be larger upon entry. It will continue to be larger until the depth at which

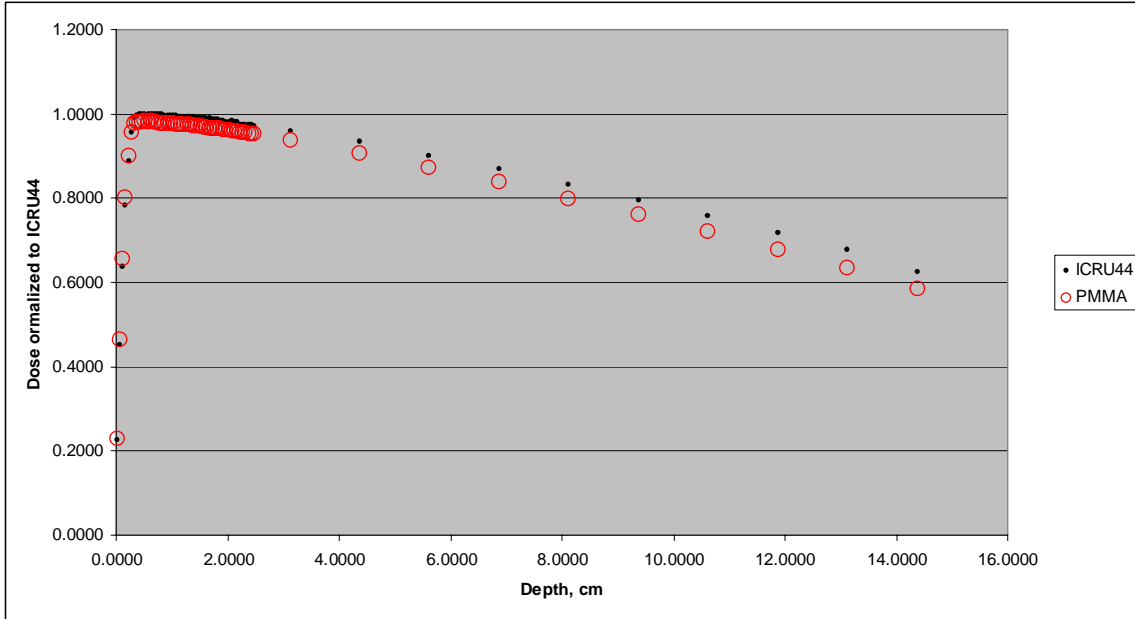


Figure 3 - Depth-dose profiles of ICRU44 and PMMA for 1.25-MeV photon, dose normalization wrt ICRU44's

its maximum dose, due to build-up, occurs, which in this particular example is the same for ICRU44. At max depth, there is less residual energy in the PMMA than there is in ICRU44 for this “1-photon” example. Thus for depths larger than that of the “max-dose depth” the dose in the PMMA will be less than that in ICRU44. This same argument can be made for PMMA in Figure 2a and 2b, where the dominate energy in the Mohan15 is in the energy region from 1.25-MeV to 1.5-MeV. As can be seen from the spectral distributions shown in Figure 4, the arguments for the particular amounts PMMA is first less and then less than that of ICRU44 with increasing depth are more complex, even though fundamentally the same than that for the 1.25-MeV case because of the spectral distribution and the different absorption associated with each energy. A similar, but reversed argument can be made for PE's lower dose at shallow depth and larger dose at larger depth.

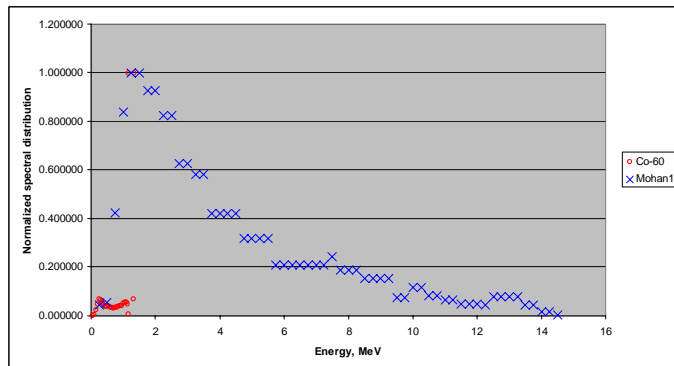


Figure 4 – Energy spectrum for Co60- and Mohan15-photon radiations

In Figures 3a and 3b the average difference in dose between for each of the two neat resins and for ICRU44 increases with decreasing depth interval from a lower depth to that of 14 cm. Values are tabulated in Table II. They represent, for the respective ranges of depth, the errors in estimated dose when the respective polymer is used as phantom material. Except for the largest interval in the case of Mohan15 photon spectra the errors are from several to almost 8 percent and would appear to not be acceptable for critical applications of radiation treatment unless a tedious process of corrections is executed.

Table II – Average percent error in dose for PE and PMMA soft-tissue phantoms

Depth interval	Cobalt 60 Photon Spectra		Mohan15 Photon Spectra	
	PE	PMMA	PE	PMMA
2.5 to 14 cm	5.77	-4.29	0.61	-3.26
5.0 to 14 cm	6.51	-4.98	2.85	-4.50
7.0 to 14 cm	7.10	-5.50	3.19	-4.68
10.0 to 14 cm	7.81	-6.03	3.43	-4.90

Figures 5a and 5b are the depth-dose profiles for A150 and Figures 6a and 6b are for TEPB1, and TEPB2 compared to that for ICRU44, for Co60 and Mohan15 photon spectra.

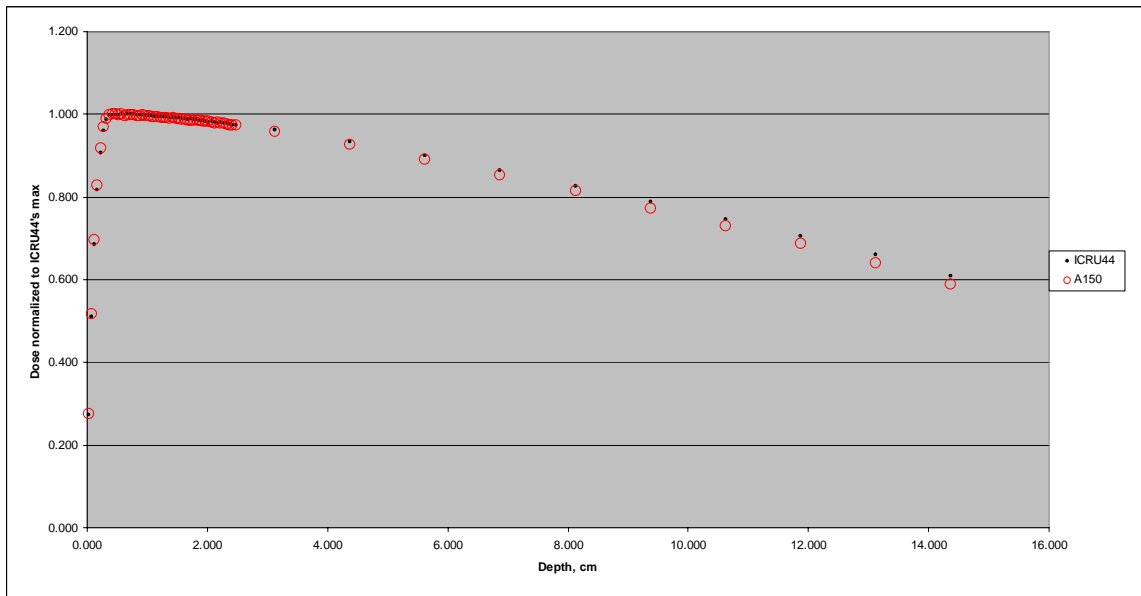


Figure 5a – Depth-dose profiles of ICRU44 and A150 for Co60 photon spectra

Visual comparison of Figures 5a and 5b to Figures 1a and 1b indicates that A150 provides much better agreement with ICRU44 than do the two neat resins, particularly at the depths at which the maximum dose, caused by build-up, occurs. So it is no wonder that Shonka’s A150 is a standard material for in ionization chambers and phantoms, and any further elaboration would be to repeat what has been long established.

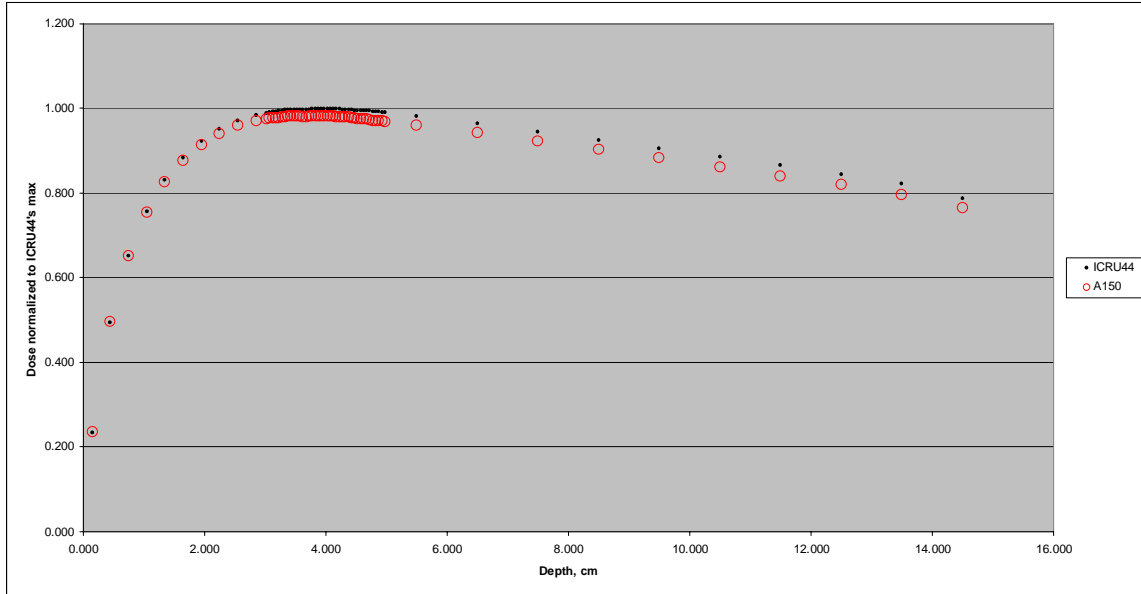


Figure 5b – Depth-dose profiles of ICRU44 and A150 for Mohan15 photon spectra

Comparisons of the depth-dose profiles in TEPB1 and TEPB2 to those in ICRU44, for Co60 and Mohan photon spectra, are provided in Figures 6a and 6b. Clearly, from visual comparison of these figures to Figures 5a and 5b, the two polymer blends have depth-dose profiles that are significantly more like those of ICRU44 than are those for A150.

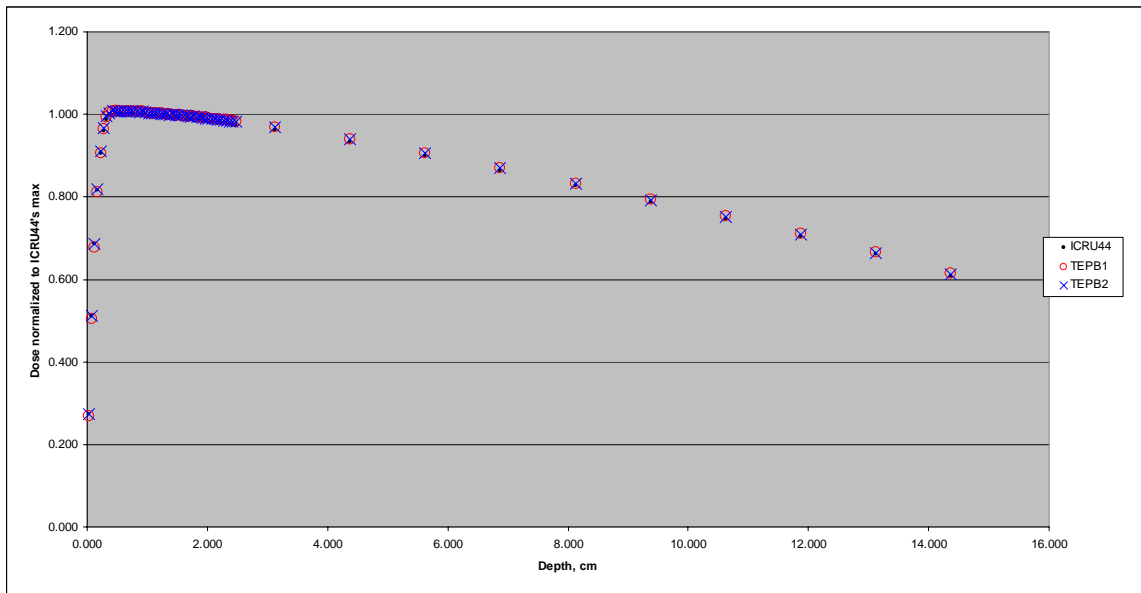


Figure 6a – Depth-dose profiles of ICRU44, TEPB1, and TEPB2 for Co60 photon spectra

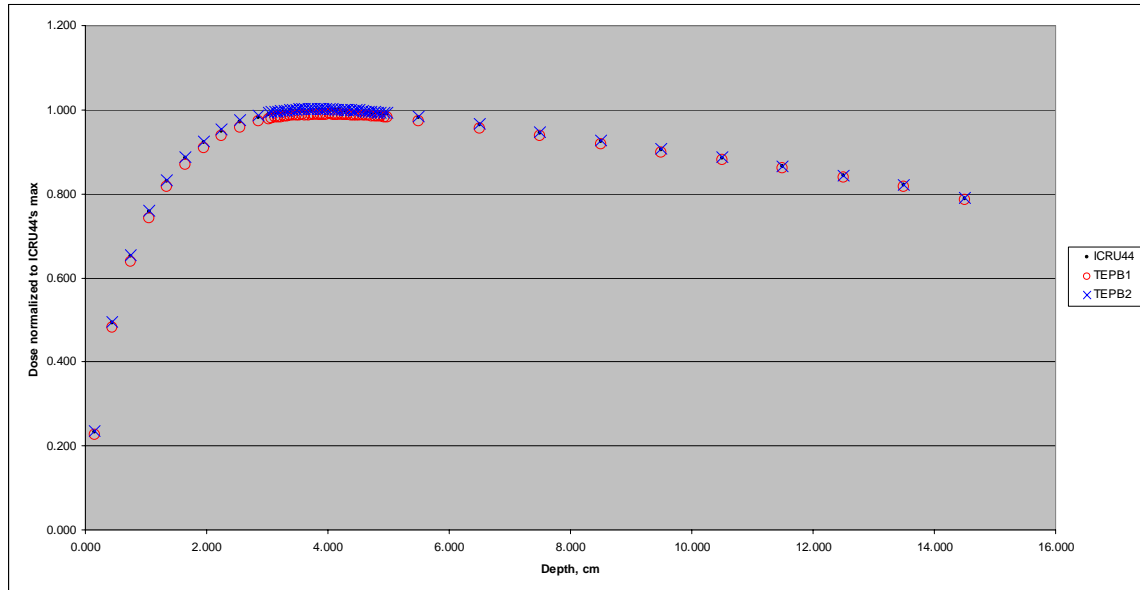


Figure 6b - Depth-dose profiles of ICRU44, TEPB1, and TEPB2 for Mohan15 photon spectra

A quantitative comparison of the two tissue-equivalent polymer blends' errors with respect to ICRU44 to those of A150 may be seen in Table III. The data in Table III is the same type as in Table II. First, A150's errors are approximately half those of PE and PMMA shown Table II. A very similar comparison of A150 to PE and PMMA can be made from the percent difference in absorption data in Table I. Note also from the values in Table III that A150's best agreement (least percent error) with ICRU44 is at depths that include the maximum-dose caused by build-up. In the regions deeper than maximum dose in an A150 phantom the agreement is poorer, i.e. the error is larger. Thus A150 probably is not an ideal material for a thick phantom representing an entire human head or torso. And, since PE and PMMA's agreements with ICRU44 are worse than A150's, see table II, neither are these neat resins appropriate for phantoms if same errors are desired.

TEPB1 and TEPB2 are significant improvements in performance compared to the two neat resins and to A150. The errors for these two materials are much smaller, particularly at depths analogous to interior cranial and torso locations of cancers. Either, but particularly TEPB2, would make excellent phantom material if they can be fabricated.

Table III – Average percent error in dose for A150, TEPB1, and TEPB2 soft-tissue phantoms

Depth Interval	Cobalt 60 Photon Spectra			Mohan15 Photon Spectra		
	A150	TEPB1	TEPB2	A150	TEPB1	TEPB2
2.5 to 14 cm	-1.57	0.80	0.65	1.12	-0.92	0.26
5.0 to 14 cm	-2.02	0.79	0.61	-2.62	-0.64	0.19
7.0 to 14 cm	-2.35	0.78	0.58	2.73	-0.59	0.18
10.0 to 14 cm	-2.71	0.82	0.55	-2.91	-0.59	0.13

The important aspect of all these data is that a comparison of the trends and relative the depth-dose errors in Tables II and III to the absorption errors in Table I indicates that similar relative performance evaluations of the two neat resins, A150, and the two blends can be made equally as well from the absorption data as made from the depth-dose data. This is important in selecting a tool for development of tissue-equivalent materials for two reasons: First, far less time and money are required to develop and use an iterative comparison application using elemental absorption data, such as was done in this study, for formulation of potential blends than is required for use of MC application codes. The core of our simple application was developed in one day and refined over a period of several weeks. It did not require an in-depth knowledge of computer programming language because it was based on the use of spreadsheets. Hence, it did not require acquiring an application capacity beyond that which ordinarily appears on any computer, Window- or Mac-based, used in an engineering or scientific environment. The MC tool we used was available at no cost, but it did require months of on-the-job experience in order to develop a familiarity leading to confident usage. A one-week training course is apparently available, at a tuition and traveling cost, but still must be followed by a period of on-the-job experience.

The second reason for the advantage of the simple absorption modeling application is that requires a fraction of the time of that of the MC modeling to examine each formulation and refine (iterate) it. The simple absorption-based application we developed required only seconds to perform an iteration. The entire iterative process, approximately 10 iterations, for each of the two blends required less than an hour. This does not count the time to check the availability of polymeric materials as part of the process for examine the reality of choosing blend constituents and other engineering and scientific information that is needed regardless of the development modeling tool. We found for the MC runs each blend required from 4 to 6 hours, for a Co60 photon spectrum, and 6 – 10 hours, for Mohan15 photon spectra. So, for the 10 iterations required to converge on a satisfactory blend would have required from 40 to 100 hours fo run time using the MC modeling tool. Our computer is a single-processor (single-core) ~~XXXXX~~ MHz system. Perhaps the run times of the MC tool would have been less had we used a dual-core or more, such as the 8-core Mac, computer.

4. – CONCLUSIONS

Two polymeric blends were developed that have absorption and depth-dose properties that are far better than those of two neat resins that are popular phantom materials and that of a current standard tissue-equivalent material. The data shows that using a simple absorption modeling tool developed for this study provided a quality of guidance that was quantitatively equal to that provided by a well-established Monte Carlo modeling tool. The absorption modeling tool provided data in seconds for each iteration in the development of a blend, approximately 10 iterations per blend, whereas each run of the MC modeling tool required from 4 to 10 hours. The absorption tool did not require any special programming or use knowledge in that it was based on the use of spreadsheets.

The MC tool required a considerable number of on-the-job hours in order to establish a level of confidence for its use in this application.

The conclusion to be drawn from the data is that the confidence for the use of a simple absorption-based modeling tool for the development of tissue-equivalent materials is equal to that for using a Monte Carlo modeling tool. Moreover, the absorption-based tool is more effective on both the basis of time and dollar costs. It requires seconds for an iteration of modeling whereas the MC tool requires hours. It also requires no particular programming or use knowledge beyond that ordinarily encountered for the use of spreadsheets. This is not to say that in the end the MC tool is not valuable, if for no other reason than it provides a confidence in the use of the use of the absorption modeling tool for development of tissue-equivalent blends of polymers. Thus the creation of these types of blends are within the means of any person who is sufficiently familiar with the fundamentals of the absorption of radiation energy. Finally, given the fact that when Shonka developed A150 Soft Tissue material not even spreadsheet applications were likely available we applaud his accomplishment.

5. - REFERENCES

1. – T. N. Padikal and S.P. Fivozinsky, Medical Physics Data Book, NBS Handbook 138.
2. Tissue Substitutes in Radiation Dosimetry and Measurement, ICRU Report 44, 1989.
3. – R. Varadhan, J Miller, B. Garrity, and M. Weber, In vivo prostate IMRT dosimetry with MOSFET detectors using brass buildup caps, Journal of Applied Clinical Medical Physics, Vol., No.4, Fall 2006.
4. - R. F. Shonka, J. E. Rose, and G. Failla, Conducting plastic equivalent to tissue, air and polystyrene, Second United Nations International Conference on Peaceful Uses of Atomic Energy. New York: United Nations, P. 160, 1958.
5. – J Burmeister, C Kota, and R. Maughan, A conducting plastic simulating brain tissue, Medical Physics, Vol. 27, Issue 11, P. 2560-2564, November 2000.
6. – R Mohan, C Chui, and L, Lidofsky, Energy Angular Distributions of Photons from Medical Linear accelerators, Med. Phys., Vol. 12, No.6, Sept/Oct 1985.
7. - D.A. Schauer, J.R. Cassata and J.J. King , A Comparison of Measured and Calculated Photon Backscatter from Dosimeter Calibration Phantoms, Radiation Protection Dosimetry, Vol. 88, P. 319-321, 2000.

8. - R.J. Traub, J.C. McDonald and M.K. Murphy , Determination of Photon Backscatter from Several Calibration Phantoms, *Radiation Protection Dosimetry*, Vol. 74, P. 13-20, 1997.

9. - P. K. Job, M. Pisharody, E. Semones, Measurement of Adsorbed Dose by 7-GeV Bremsstrahlung in a PMMA Phantom, *Nucl. Instrum. Methods A*. 438, 540 (1999)

10. – Nuclear Associates Model 84-057

<http://www.supertechx-ray.com/a2120-r.htm>

11. - Harold E. Kim, Mary Ann Krug, Inn Han, John Ensley, George H. Yoo, Jeffrey D. Forman and Hyeong-Reh Choi Kim² , Neutron Radiation Enhances Cisplatin Cytotoxicity Independently of Apoptosis in Human Head and Neck Carcinoma Cells¹ , *Clinical Cancer Research* Vol. 6, P. 4142-4147, October 2000

12.- A. Kosunen, M. Kortensniemi, H. Ylä-Mella, T. Seppälä, J. Lampinen, T. Serén, I. Auterinen, H. Järvinen and S. Savolainen , Twin Ionisation Chambers for Dose Determinations in Phantom in an Epithermal Neutron Beam, *Radiation Protection Dosimetry* 81:187-194 (1999)

13. - M. Yudelev, K. Alyousef, J. Brandon, V. Perevertailo, M. L. F. Lerch and A. B. Rosenfeld , Application of semiconductors for dosimetry of fast-neutron therapy beam, *Radiation Protection Dosimetry* 110(1-4):573-578 2004

14. - I H Ferreira, C E de Almeida, D Marre, M H Marechal, A Bridier† and J Chavaudra, Monte Carlo calculations of the ionization chamber wall correction factors for ¹⁹²Ir and ⁶⁰Co gamma rays and 250 kV x-rays for use in calibration of ¹⁹²Ir HDR brachytherapy sources, *Phys. Med. Biol.*, Vol 44. P. 1897-1904, 1999

15. - H J Brede, D Schlegel-Bickmann, G Dietze, J Daures-Caumes and A D Ostrowsky, Determination of absorbed dose within an A150 plastic phantom for a d(13.35 MeV)+Be neutron source, *Phys. Med. Biol.*, Vol. 33, P. 413-425, 1988

16. - Masashi Takada, Erika Mihara, Takashi Nakamura, Toshihiko Honma, Koji Kono and Kazunobu Fujitaka, Neutron irradiation field produced by 25 MeV deuterons bombarding on thick beryllium target for radiobiological study , *Nuclear Instruments and Methods in Physics Research Section A: Accelerators, Spectrometers, Detectors and Associated Equipment* Volume 545, Issue 3, 21, P. 765-775, June 2005

17. - <http://www.orau.org/ptp/collection/ionchamber/shonkatissueequivalent.htm>

A polymer-based composite material is a good choice for large structures such as wind turbine blades. The high strength-to-density ratio, high stiffness-to-density ratio, good fracture toughness, fatigue performance and suitability for use in fast production of large structures makes composites a good choice for their use in structural applications. The composite properties provided by the manufacturer are generally the average properties in a particular manufacturing environment. On top of this, manufacturers usually don't mention the number of tests that they performed to obtain the average. This led to the creation of hybrid materials composed of polymer matrices and carbon additives. Pioneering publications on polymer nanocomposites appeared in the early 1990s. Despite the broad use of polymer composites with carbon additives, the annual number of papers did not significantly change from 2005 to 2016 (except publications on polymer ± PCBM composites whose number has been increasing dramatically over the last years). The groundbreaking experiments on graphene by A. Geim and K. Novoselov, which resulted in the 2010 Nobel Prize in physics, provide a renewed perspective on the application of carbon nanoparticles and nanoscience in general. This allowed for the creation of a bulk heterojunction (BHJ)-based solar cells where the semi 2 Opportunities for Polymeric-Based Composite Applications for Transport Aircraft. 2.1 Emerging New Aircraft Have the Most Efficient Structures. 2.2 Impact Considerations. References. 3 Composite Materials for Marine Applications: Key Challenges for the Future. 3.1 Introduction. 3.2 Load Transfer Mechanisms. 3.3 Safety. 3.4 Life Cycle Assessment. 3.5 Concurrent Engineering. 6.2 Design Principles and Testing of Wear Resistant Polymer Composites. 6.3 General Aspects of Friction and Wear of Nano-particle Modified Polymer Composites. 6.3.1 Incorporation of Nano-particles into Polymeric Matrices. 6.3.2 Synergistic Effects of Nano-particles and Traditional Fillers on the Sliding Wear of Different Polymer-Based Composites. The possibilities are immense for using BNNT for multifunctional radiation shielding structural materials for future space exploration architectures. This early study is focused on a visionary aerospace concept. This is an architecture or systems concept, currently at TRL = 1-2 in maturity, aiming 10 or more years in the future. The computer code used was OLTARIS (On-Line Tool for the Assessment of Radiation in Space) (Ref. 4). OLTARIS is an integrated tool set utilizing the HZETRN (High Charge and Energy Transport) code developed at the NASA Langley Research Center. These tools are intended to help scientists and engineers study the effects of space radiation on shielding materials, electronics, and biological systems.